Acta Cryst. (1997). D53, 125–128

Crystallization and preliminary X-ray analysis of tobacco ringspot virus

VEDA CHANDRASEKAR,[a,b] SANJEEV MUNSHI[b] AND JOHN E. JOHNSON[a]* *at* [a]*Department of Molecular Biology, MB-13, The Scripps Research Institute, 10550 North Torrey Pines Road, La Jolla, CA 92037, USA, and* [b]*Department of Biological Sciences, Structural Biology Group, Purdue University, West Lafayette, IN 47907, USA. E-mail: jackj@scripps.edu*

(Received 8 July, 1996; accepted 17 September, 1996)

Abstract

Tobacco ringspot virus, a plant virus that is believed to fill an apparent niche in the evolution of picornavirus-like capsids, has been crystallized by vapor diffusion with potassium phosphate and polyethylene glycol buffered at pH 6.5 in a new crystal form. The monoclinic crystals belong to the space group $C2$ with unit-cell dimensions of $a = 407.1$, $b = 399.7$, $c = 285.9$ Å and $\beta = 129.1°$ and diffract synchrotron radiation to 3.3 Å. One half of a virus particle constitutes the crystallographic asymmetric unit. The orientation of the virus particle in the unit cell was determined by the rotation function analysis of a partial data set that has been collected at CHESS using image plates. Development of a suitable phasing model for the high-resolution structure determination of TRSV with the real-space molecular replacement technique is now under way.

1. Introduction

Tobacco ringspot virus (TRSV), a small RNA plant virus, is the type member of the nepovirus group (Harrison & Murant, 1977; Stace-Smith, 1985). Viruses belonging to this group are numerous and cause important diseases of various soft fruits, including the grapevine fanleaf disease. Some of the members include arabis mosaic, grapevine fanleaf, tomato blackring, cherry leafroll and tomato ringspot viruses. Nepoviruses have a wide host range and are believed to be transmitted by the adult and larval stages of the soil-inhabiting nematodes, by sap inoculation and the seed of infected plants. Other insect vectors may also be involved.

TRSV causes soybean budblight, ringspot diseases of tobacco and cucumber, and chlorotic or necrotic spotting in many annual and perennial crops. The TRSV genome is bipartite and consists of two positive-sense single-stranded RNA molecules of 2.6×10^6 Da (RNA1) and 1.2×10^6 Da (RNA2) that are encapsidated separately in polyhedral particles of 280 Å diameter (Diener & Schneider, 1966; Murant, Taylor, Duncan & Raschke, 1981). Both types of particles are required for infection. A third particle containing no RNA has been detected in infected plants. Small satellite RNA molecules which depend upon the genomic RNA molecules of TRSV for the coat protein and for replication functions have been detected in some isolates of the virus (Schneider, 1971). RNA1 and RNA2 possess a genome-linked protein (VPg) covalently linked to the 5′ terminus (Mayo, Baker & Harrison, 1979*a*) and a polyadenylate tract at the 3′ end (Mayo *et al.*, 1979*b*). The genome-linked protein is essential for virus infectivity. The RNA1 encodes the RNA polymerase, a protease, VPg and a putative helicase with a NTP binding site. All four of these proteins are involved in the virus replication. The RNA2 encodes the capsid protein and an upstream putative movement protein (Jobling & Wood,1985; Forster & Morris-Krsinich, 1985). The TRSV particle shell is composed of 60 identical subunits of the capsid protein (56 000 *MW*; 513 amino acids; Mayo, Murant & Harrison, 1971; Buckley, Silva & Singh, 1993, 1995) arranged in a $T = 1$ ($P = 3$, *i.e.* pseudo $T = 3$) lattice (Caspar & Klug, 1962).

Icosahedral RNA virus particles composed of 180 β-barrel domains (the common fold found in most viral subunits) fall into two categories. The $T = 3$ particles in which all the β-barrel domains are the same gene product, and the picornavirus-like capsids in which there are 60 copies of three β-barrel domains with distinct amino-acid sequences. The three β-barrel domains in the latter particle are synthesized as a polyprotein. The plant virus groups of nepoviruses and comoviruses are classified in the picornavirus supergroup based on the similarities in the organization of the genes in the genomic RNA, expression of the genomic RNA as a polyprotein and the subsequent post-translational cleavage of the polyprotein by a virally encoded protease, and the sequence similarity among the non-structural proteins (like RNA polymerase) to animal picornaviruses (Goldbach & Wellink, 1988). It is to be noted that there is not much sequence similarity that is statistically significant among the capsid polyproteins of nepoviruses, comoviruses and picornaviruses. In picornaviruses the capsid polyprotein is cleaved into three separate β-barrel domains, VP1, VP2 and VP3. Comoviruses contain only one cleavage site in the capsid polyprotein and the shell is composed of 60 copies each of a large (VP2 + VP3) and a small (VP1) protein. It has been proposed that there are no cleavage sites in the nepovirus capsid polyprotein and that all the three domains have remained covalently linked as a polyprotein in the capsid. Since picornavirus capsids may have evolved from $T = 3$ particles by gene triplication, followed by the development of cleavage sites, nepoviruses may be the most primitive of the picornavirus-like capsids, lacking any of the cleavage sites. The capsid protein architecture observed in the high-resolution structures of comoviruses and picornaviruses is similar (Rossmann & Johnson, 1989). We are pursuing the high-resolution structural studies of TRSV to see if the locations of the three domains in the TRSV capsid protein agree with the consensus precursor of picorna- and comovirus capsids. The structure will be useful not only in the understanding of the nepovirus group of plant viruses but also in providing a scope for detailed structural comparisons with the already available high-resolution structures of a number of comoviruses and picornaviruses. Correlation of this structural information of TRSV with the assembly and packaging studies being carried out using a baculovirus expression system (Sing, Rothnagel,

† Present address: WP44-B122, Merck Research Laboratory, Lansdale, PA 19486, USA.

Prasad & Buckley, 1995) should lead to a better understanding of viruses like TRSV that are stabilized by protein–protein interactions.

2. Methods and materials

2.1. *Virus purification*

TRSV was propagated in tobacco plants (*Nicotiana tabacum* cv. Xanthi - nc) and purified according to the method reported by Rezian & Francki (1973) with some modifications as summarized below. TRSV was purified by a combination of PEG precipitation and ultracentrifugation. Infected tobacco leaves were frozen at 253 K, crushed and homogenized with the homogenization buffer [0.1 *M* potassium phosphate, pH 7, with 0.01 *M* EDTA and 0.4%(*v*/*v*) β-mercaptoethanol] in a Waring blender. The homogenate was centrifuged at 9000 rev min^{-1} for 25 min to pellet the leaf tissue. Chloroform and *n*-butanol were added to the supernatant fluid (in the ratio of 1:1:2 by volume). The mixture was kept at 277 K for 30 min and centrifuged at 8000 rev min^{-1} for 15 min. The aqueous amber layer containing the virus was collected by aspiration and the virus was precipitated by the addition of 8% PEG (*MW*8000) and 0.2 *M* sodium chloride. The virus precipitate was pelleted by low-speed centrifugation and resuspended in 0.1 *M* potassium phosphate, pH 7, with 0.01 *M* EDTA. The resuspension was clarified and the virus was pelleted by centrifugation at 42 000 rev min^{-1} for 2 h. The virus pellet was resuspended in the storage buffer (0.1 *M* potassium phosphate, 1 m*M* sodium azide, pH 7) prior to crystallization. All purification steps were performed at 277 K. Yields of 20–40 mg of TRSV per kg of leaf tissue were typical. Virus purity was determined by polyacrylamide gel electrophoresis under denaturing conditions for the coat protein and by UV spectrophotometry ($E_{260}^{1\text{mg ml}^{-1}} = 8.0$; $A_{260}/A_{280} = 1.7$). The virus particles sediment as three components with Svedberg coefficients of 53S, 91S and 126S for the top, middle and bottom components, respectively (Stace-Smith, 1985). The virus samples used for crystallization were not subjected to gradient separation after purification.

2.2. *Crystallization*

Large unit-cell dimensions and fragility of the previously studied single crystals (Huess, Murthy & Argos, 1981) has hindered the structure determination of TRSV. The crystallization conditions were modified from those previously published by altering the molecular weight of the precipitant (PEG) used to get a new crystal form of TRSV. The virus was crystallized using the sitting-drop method of vapor diffusion (McPherson, 1982). The reservoir buffer was 0.125 *M* potassium phosphate, 2–3%(*w*/*v*) PEG 3350, 1 m*M* sodium azide, pH 6.5. The crystallization droplet consisted of 5–25 µl of TRSV in storage buffer at 20 mg ml^{-1} added to an equal volume of reservoir buffer. This mixture was allowed to equilibrate at room temperature against 15 ml of reservoir buffer. Monoclinic crystals grew to a size of 0.2–0.4 mm in two to four weeks.

2.3. *Data collection, processing and rotation function*

A partial data set from 50.0 to 3.3 Å resolution was collected using Fuji image plates on the F1 beamline at the Cornell High Energy Synchrotron Source (CHESS). Monochromatic radiation ($\lambda = 0.91$ Å) was used to record 0.3° oscillation photographs with a crystal-to-film distance of 300 mm and exposure time of 20 s. The image plates were scanned on a Fuji BAS3000 scanner with a 100 µm raster step. The unit-cell parameters were estimated using the program *DENZO* (Otwinowski, 1993). The crystal orientation relative to the camera coordinate system was determined by an indexing program developed by Kabsch (1988). The orientation matrix from this program was used in the film processing package *OSC* developed by Rossmann (1979) to measure the diffraction intensities. The data were scaled and postrefined to get better estimates of cell dimensions, crystal setting, crystal mosaicity and partiality of the reflections (Rossmann, Leslie, Abdel-Meguid & Tsukihara, 1979). A self-rotation function on the processed data was computed using the Rossmann–Blow algorithm (Rossmann & Blow, 1962) to determine the orientation of the icosahedral non-crystallographic symmetry elements with respect to the crystal axes.

3. Results and discussion

3.1. *Crystal analysis and data processing*

The crystals remained stable in vapor-diffusion growth chambers at room temperature and diffracted synchrotron radiation to at least 3.5 Å. An initial estimate of the unit-cell parameters were obtained using the autoindexing program *DENZO* which indicated a *C*-centered monoclinic lattice with unit-cell parameters of $a = 408.5$, $b = 399.7$, $c = 286.9$ Å and $\beta = 129.1°$ and *C*2 space-group symmetry. Attempts to define a unit cell with higher symmetry (including a rhombohedral cell) were unsuccessful. The predicted diffraction patterns in these cases did not match the observed diffraction pattern very well.

The presence of *C*-centering in the lattice was confirmed by the nearly zero or negative intensity values for any general observed reflection *hkl* with $(h + k)$ being odd. For the *C*2 symmetry-related reflections found on the same image plate *R* factors* of 15% or lower were observed. The diffraction data measured from 71 individual image plates were combined and scaled. The statistics for scaling and postrefinement and the percentage of measured unique reflections as a function of resolution are shown in Table 1.

3.2. *Rotation-function analysis*

Volume per molecular weight (V_m; Matthews, 1968) calculations can be used to estimate the number of virus particles per unit cell. A V_m value of 3.2 Å^3 Da^{-1} for TRSV indicated that there were two virus particles per unit cell. The two particles related by *C* centering were positioned at (0,0,0) and ($\frac{1}{2}$, $\frac{1}{2}$, 0) and were in the same orientation. This implied that one of the icosahedral twofold axis of the virus particle must coincide with the crystallographic twofold axis (*b* axis). Therefore, the particles had rotational freedom only about this twofold axis and the rotation-function search was essentially reduced to a one-dimensional search. This also resulted in 30-fold non-crystallographic symmetry. Self-rotation functions were computed to search for peaks in the rotation function about the crystallographic twofold axis. The spherical polar coordinate convention (as defined by Rossmann & Blow,

* R factor $= [\sum_h \sum_i (I_{hi} - I_h) / \sum_h \sum_i I_h] \times 100$ where I_h is the mean intensity of the i observations of the reflection h with intensities I_{hi}.

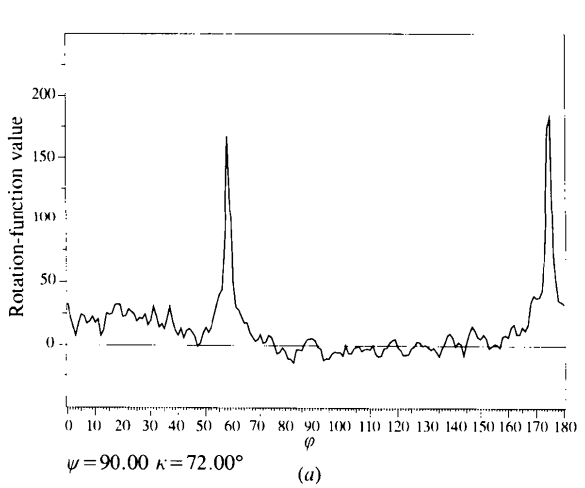

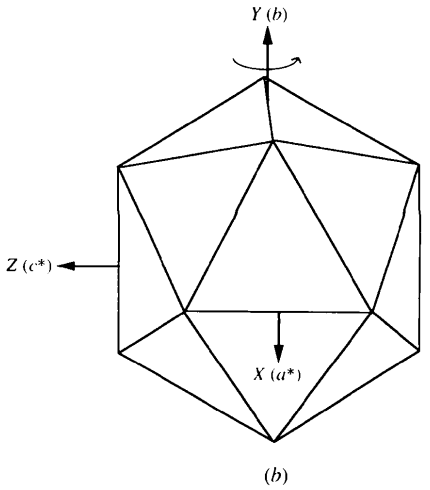

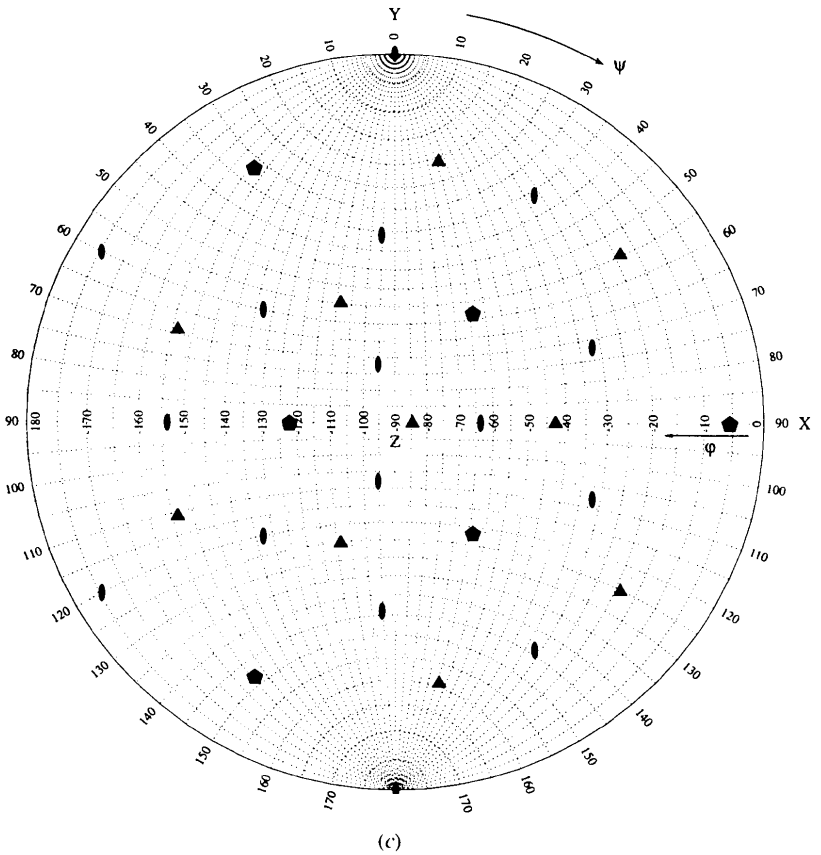

Fig. 1. (*a*) One-dimensional self rotation function for TRSV (with $\kappa = 72°$ for the fivefold axis search, $\psi = 90°$ and φ ranging from 0 to 180°) computed with the partial data set between 10 and 8 Å resolution and a radius of integration of 140 Å. A total of 1614 'large terms' (representing 33% of the measured data in the resolution range) were used to represent the second Patterson function. The positions of the two peaks observed indicated that the virus particle was rotated by 26° about the *Y* axis with respect to the standard orientation defined in (*b*). (*b*) An icosahedron in the standard orientation in which a set of three orthogonal icosahedral twofold axes coincide with the *X*, *Y* and *Z* axes. The *Y* axis coincides with the crystallographic twofold axis (*b* axis). In going from the *X* to the *Y* axis the icosahedral symmetry axes encountered will be in the order twofold axis–threefold axis–fivefold axis–twofold axis. The direction of rotation of 26° about the *Y* axis observed in the rotation-function analysis of TRSV is indicated by the arrow (the twofold axis along the *Z* axis in the standard orientation is rotated towards the *X* axis by 26°). (*c*) A stereographic projection of the constellation of the icosahedral symmetry elements for the TRSV particle in the monoclinic cell. The *Z* axis projects out of the page and coincides with the *c** direction. The *Y* axis is along the *b* axis. The fivefold, threefold and the twofold axes are depicted as pentagons, triangles and ovals, respectively. The one-dimensional search shown in (*a*) corresponds to the central line (with $\psi = 90°$) here. Also note that the φ angle ranges from 0 to $-180°$ and the pentagons seen at $\varphi = -5°$ and $\varphi = -122°$ correspond to the peaks observed at $\varphi = 175°$ and $\varphi = 58°$ in (*a*), respectively.

Table 1. *Summary of the number of reflections measured after scaling 71 imaging plates from 26 crystals of TRSV*

The diffraction data was processed in the $C2$ space group with unit-cell parameters of $a = 408.5$, $b = 399.7$, $c = 286.9$ Å and $\beta = 129.1°$. The option 1 scaling R factor for only whole reflections with $I \geq 4\sigma(I)$ was 10.84% (64710 total observations, 57600 unique reflections). After post refinement the cell parameters refined to $a = 407.1$, $b = 399.7$, $c = 285.9$ Å and $\beta = 129.1°$. The horizontal and vertical mosaicity refined to 0.1806 and 0.1485 from their starting value of 0.105 used to process the data. After postrefinement the option 1 scaling R factor for only whole reflections with $I \geq 4\sigma(I)$ was 8.4% (40649 total observations, 37381 unique reflections). The final scaling R factor for whole and partial reflections with partiality greater than 0.5 and $I \geq 4\sigma(I)$ was 10.3% (113018 total observations, 92395 unique reflections).

Resolution range (Å)	No. of unique reflections	% Theoretically observable data
50–30	117	16
30–20	380	22
20–10	4045	24
10–8	4769	26
8–6	12913	26
6–5	15710	24
5–4	28660	20
4–3.5	14332	10
3.5–3.3	11469	4
Total	92395	13

1962) was used to define the search angles. The rotation function computed with $\kappa = 72°$ to search for the fivefold non-crystallographic symmetry axes directions is shown in Fig. 1(*a*). The peaks observed indicated that the virus particle was rotated by $26 \pm 0.5°$ about the crystallographic twofold axis with respect to the standard virus orientation defined in Fig. 1(*b*). The precise value of the rotation was narrowed down to $\kappa = 26.3 \pm 0.05°$ by performing finer searches using the observed intensity data between 6.0 and 5.0 Å resolution. Self-rotation functions were also computed with $\kappa = 120°$ and $\kappa = 180°$ to search for the orientation of the threefold and twofold non-crystallographic symmetry axes to confirm the result from the fivefold search.

These results were confirmed by computing a locked self-rotation function (Tong & Rossmann, 1990) which enhances the power of the rotation-function search performed on an incomplete data set. A one-dimensional locked self-rotation search was computed about the crystallographic twofold axis (by fixing $\varphi = 0°$ and $\psi = 0°$) and rotating by an angle κ. A broad search was performed for $\kappa = 0$–$180°$ at 1° intervals. The search used 560 large terms between 10.0 and 8.0 Å resolution with a radius of integration of 140 Å. A single large peak of 7.9σ was observed in the rotation function at $\kappa = 26°$. The location of the icosahedral symmetry operators determined by this search (Fig. 1*c*) was consistent with the peaks observed in the self-rotation searches (Fig. 1*a*).

A more complete data set to 3.3 Å will be collected shortly. Meanwhile, phasing attempts by the molecular replacement technique have been initiated (Rossmann, 1990). The cowpea mosaic virus (CPMV), a comovirus with the three-dimensional structure solved to 3.0 Å resolution (Chen, Stauffacher & Johnson, 1990) will be used as the model because of the evident evolutionary link between the nepoviruses and comoviruses. The CPMV polyalanine model will be fitted into the electron-density map corresponding to the three-dimensional reconstruction of TRSV to 22 Å resolution determined from the cryo-electron microscopy images of the TRSV VLP's that formed when the capsid polyprotein of TRSV was expressed in a baculovirus expression system (Singh *et al.*, 1995). The strategy of averaging the electron-density map over the 30-fold non-crystallographic symmetry and solvent flattening will be used to refine the phases at a given resolution and phase extension will be carried out gradually to the highest resolution permitted by the data set.

We thank Bonnie Mckinney, Tim Schmidt, Dr Tianwei and the staff at CHESS for assistance in data collection. The research was supported by a grant from the National Institutes of Health R01 GM 54076.

References

Buckley, B., Silva, S. & Singh, S. (1993). *Virus. Res.* **30**, 335–349.

Buckley, B., Silva, S. & Singh, S. (1995). *Virus. Res.* **35**, 111.

Caspar, D. L. D. & Klug, A. (1962). *Cold Spring Harbor Symp. Quant. Biol.* **27**, 1–24.

Chen, Z., Stauffacher, C. V. & Johnson, J. E. (1990). *Semin. Virol.* **1**, 453–466.

Diener, T. O. & Schneider, I. R. (1966). *Virology*, **29**, 100–105.

Forster, R. L. S. & Morris-Krsinich, B. A. M. (1985). *Virology*, **144**, 516–519.

Goldbach, R. & Wellink, J. (1988). *Intervirology, 29*, 260–267.

Harrison, B. D. & Murant, A. F. (1977). *Nepovirus group, CMI/AAB Descriptions of Plant Viruses, No. 185.* Commonwealth Mycological Institute and Association of Applied Biologists, Surrey, England.

Huess, K. L., Murthy, M. R. N. & Argos, P. (1981). *J. Mol. Biol.* **153**, 1161–1168.

Jobling, S. A. & Wood, K. R. (1985). *J. Gen. Virol.* **66**, 2589–2596.

Kabsch, W. (1988). *J. Appl. Cryst.* **21**, 67–71.

McPherson. A. (1982). *The Preparation and Analysis of Protein Crystals.* New York: John Wiley.

Matthews, B. W. (1968). *J. Mol. Biol.* **33**, 491–497.

Mayo, M. A., Baker, H. & Harrison, B. D. (1979*a*). *J. Gen. Virol.* **43**, 603–610.

Mayo, M. A., Baker, H. & Harrison, B. D. (1979*b*). *J. Gen. Virol.* **43**, 735–740.

Mayo, M. A., Murant, A. F. & Harrison, B. D. (1971). *J. Gen. Virol.* **12**, 175–178.

Murant, A. F., Taylor, M., Duncan, G. H. & Raschke, J. H. (1981). *J. Gen. Virol.* **53**, 321–332.

Otwinowski, Z. (1993). *DENZO.* In *Data Collection and Processing.* Warrington: Daresbury Laboratory.

Rezian, M. A. & Francki, R. I. B. (1973). *Virology*, **56**, 238–249.

Rossmann, M. G. (1979). *J. Appl. Cryst.* **12**, 225–238.

Rossmann, M. G. (1990). *Acta Cryst.* **A46**, 73–82.

Rossmann, M. G. & Blow, D. M. (1962). *Acta Cryst.* **15**, 24–31.

Rossmann, M. G. & Johnson, J. E. (1989). *Annu. Rev. Biochem.* **58**, 533–573.

Rossmann, M. G., Leslie, A. G. W., Abdel-Meguid, S. S. & Tsukihara, T. (1979). *J. Appl. Cryst.* **12**, 570–581.

Schneider, I. (1971). *Virology*, **45**, 108–122.

Singh, S., Rothnagel, R., Prasad, B. V. & Buckley, B. (1995). *Virology*, **213**, 472–481.

Stace-Smith, R. (1985). *Tobacco ringspot virus, CMI/AAB Descriptions of Plant Viruses, No. 309.* Commonwealth Mycological Institute and Association of Applied Biologists, Surrey, England.

Tong, I. & Rossmann, M. G. (1990). *Acta Cryst.* **A46**, 783–792.